DNA Shuffling of Adeno-associated Virus Yields Functionally Diverse Viral Progeny

James T Koerber[1–3], Jae-Hyung Jang[1–3] and David V Schaffer[1–3]

[1]Department of Chemical Engineering, University of California at Berkeley, Berkeley, California, USA; [2]Department of Bioengineering, University of California at Berkeley, Berkeley, California, USA; [3]Helen Wills Neuroscience Institute, University of California at Berkeley, Berkeley, California, USA

Adeno-associated virus (AAV) vectors are extremely effective gene-delivery vehicles for a broad range of applications. However, the therapeutic efficacy of these and other vectors is currently limited by barriers to safe, efficient gene delivery, including pre-existing antiviral immunity, and infection of off-target cells. Recently, we have implemented directed evolution of AAV, involving the generation of randomly mutagenized viral libraries based on serotype 2 and high-throughput selection, to engineer enhanced viral vectors. Here, we significantly extend this capability by performing high-efficiency *in vitro* recombination to create a large (10^7), diverse library of random chimeras of numerous parent AAV serotypes (AAV1, 2, 4–6, 8, and 9). In order to analyze the extent to which such highly chimeric viruses can be viable, we selected the library for efficient viral packaging and infection, and successfully recovered numerous novel chimeras. These new viruses exhibited a broad range of cell tropism both *in vitro* and *in vivo* and enhanced resistance to human intravenous immunoglobulin (IVIG), highlighting numerous functional differences between these chimeras and their parent serotypes. Thus, directed evolution can potentially yield unlimited numbers of new AAV variants with novel gene-delivery properties, and subsequent analysis of these variants can further extend basic knowledge of AAV biology.

Received 28 February 2008; accepted 9 July 2008; published online 26 August 2008. doi:10.1038/mt.2008.167

INTRODUCTION

Viral gene-delivery vehicles, and particularly adeno-associated virus (AAV), have demonstrated potential to treat a range of inherited and acquired genetic disorders successfully.[1–3] AAV is a nonpathogenic member of the *Parvoviridae* family, with a single-stranded DNA genome, and mediates long-term gene expression following transgene delivery into both dividing and nondividing cells.[4–6] The viral gene *cap* encodes three structural proteins (VP1-3), which assemble as a 60-mer into an icosahedral capsid that encapsulates the viral DNA.[7]

To date, over 100 AAV genotypes have been isolated from various species, including goat, cow, nonhuman primates, and humans.[8,9] The sequence variability within the viral capsid underlies an extensive range of gene-delivery properties, such as tissue tropism and biodistribution.[10–14] Despite this extensive range of gene-delivery properties, existing AAV serotypes transduce some therapeutically desirable cell types poorly and can be strongly neutralized by pre-existing immunity.[2,15,16]

Efforts to engineer the AAV capsid for targeted delivery, which have most often relied upon sequence analysis and rational peptide insertion have enjoyed some success.[17–19] Other efforts to generate AAV variants with novel functions include combining functional regions from distinct AAV serotypes through rational domain swapping, innovative but relatively small-scale *in vivo* recombination, and co-transfection of two *cap* genes to create mosaic viruses.[20–22] However, while they exhibit novel properties, engineered variants and chimeras require some additional improvement to meet the needs of some therapeutic applications, and there is often insufficient knowledge of viral structure–function relationships to enable additional rational design of vectors.

Directed evolution is a powerful protein engineering approach that can enhance pre-existing functions of, or generate novel functions in, a protein in the absence of underlying mechanistic knowledge.[23–28] Previously, we reported a directed evolution approach, based on high-throughput random point mutagenesis and selection, that successfully generated AAV2 vectors with novel gene-delivery properties.[29] Recently, family shuffling has been used to generate chimeric AAV variants; however, the functional diversity of capsids, particularly with regard to cell tropisms and antibody evasion, present with the libraries was only minimally explored.[30,31]

Here, we extend the capabilities of AAV-directed evolution and implement *in vitro* recombination of numerous AAV serotypes to yield viral chimeras that meld the properties of their parents, and thereby exhibit gene-delivery characteristics that no existing serotype possesses. Specifically, we have generated a shuffled AAV library composed of *cap* genes from AAV1, 2, 4–6, 8, and 9. We analyzed the *cap* sequences of the library at various stages of this process—including the initial library, following viral packaging, and after infection—to probe its functional diversity. After selection for viral packaging and cellular infection, we isolated novel variants that exhibit altered cellular tropism both *in vitro* and *in vivo* and exhibit significantly enhanced

Correspondence: *David V. Schaffer, Department of Chemical Engineering, University of California, Berkeley, California 94720-1462, USA. E-mail: schaffer@berkeley.edu*

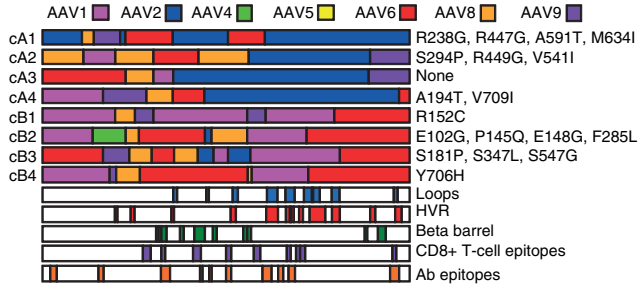

Figure 1 Amino acid sequences of shuffled clones. Graphical representations of the primary protein sequences of each chimera are shown, with the protein segments colored to reflect the parent serotypes from which they were derived. Point mutations present within each sequence are shown next to each clone. Graphical representation of several key viral regions, including surface loops,[38,46,47] hypervariable regions (HVRs),[8] β-barrel core,[38] CD8+ T-cell epitopes,[50] and antibody (Ab) epitopes,[15,16] are also depicted to highlight the diversity within these regions. AAV, adeno-associated virus.

resistance to human intravenous immunoglobulin (IVIG) compared to any of their parents, further demonstrating the functional diversity of this shuffled library. Finally, analysis of these variants yields novel insights into viral sequence–function relationships, particularly involving surface loop swapping among AAV serotypes.

RESULTS

Library construction and production

To construct the AAV library, the *cap* genes from AAV serotypes 1, 2, 4–6, 8, and 9 were subjected to DNA shuffling as previously described[23,32] and cloned into an AAV genomic plasmid,[29] resulting in $>10^7$ independent clones (*i.e.*, bacterial colonies). Sequence analysis of the numerous full-length *cap* genes revealed multiple recombination events, and every parental serotype was represented (**Supplementary Figure S1**). Specifically, for the sample set (n = 9) there were ~10.5 crossovers/chimera and an error rate comparable to other DNA shuffling protocols at ~0.37%.[23,32]

The plasmid library was used to package replication-competent AAV (rcAAV)[29] to yields that were only approximately fivefold lower than wild-type AAV2. Our initial goal was to determine the extent to which highly diverse, chimeric AAV variants can even be infectious. To enrich for "viable" clones, the viral library was added to HEK293 cells at a low genomic multiplicity of infection, followed by addition of wild-type adenovirus serotype 5. Sequence analysis of the resulting *cap* clones confirmed the presence of numerous, highly diverse chimeras (**Figure 1** and **Supplementary Figures S2** and **S3**). Importantly, no full-length wild-type AAV sequences were recovered at any stage (after shuffling, packaging, or infection).

Four clones with sequences somewhat closely related to AAV2, and four related to AAV1/6, were chosen for further analysis. Protein sequence comparison revealed similarities to AAV2 of 91.8–96% for chimeras cA1–4, and similarities to AAV1/6 of 96.4–98.3% for chimeras cB1–4. Most importantly, the VP3 sequence of these chimeras, which encompasses most of the exposed capsid surface, contained regions from multiple parents, with 24.8–53.5% of the VP3 region from cA1–4 chimera originating from non-AAV2 parents and 1.1–22.5% of the VP3 region from cB1–4 chimera originating from non-AAV1/6 serotypes. Strikingly, capsid structure representations of each chimera confirm the presence of regions from multiple serotypes on the viral surface (**Figure 2**).

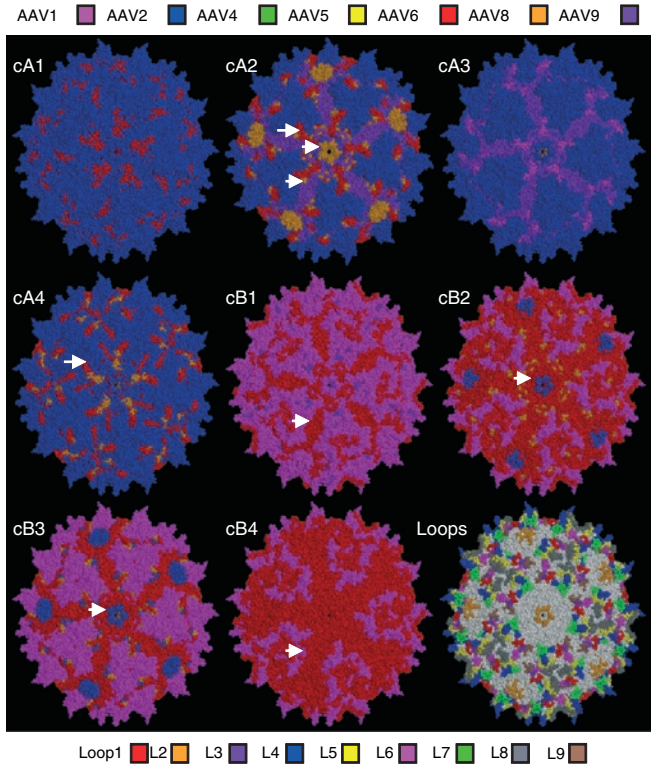

Figure 2 Structural comparison of selected viral chimeras. Molecular models of the adeno-associated virus (AAV) capsid, based on the AAV2 structure,[38] are shown for each chimera along with a model depicting the location of each loop region. Each region is shaded according to the parent serotype from which it was derived, highlighting the substantial sequence variability on exterior regions of the capsid. White arrows indicate important structural regions discussed in text.

Because DNA sequencing is a relatively low-throughput method to analyze clones from such a diverse library, we confirmed the presence of additional chimeras from the other parents (*i.e.*, AAV4, 5, 8, and 9) using a PCR screen based on specific primer sets designed to amplify a hypervariable region within the *cap* gene (corresponding to hypervariable regions of VP3) of each serotype (**Figure 3** and **Supplementary Table S1**). Hence, additional selection on other cell types or *in vivo* would likely result in the emergence of additional variants with contributions from all of the original AAV parents.

Transduction analysis

To determine whether diversity in the chimera surface regions translates to differences in viral function, recombinant AAV (rAAV) Luc vectors were produced with each chimeric capsid at titers similar to the parental viruses (AAV1, 2, 6, 8, and 9) (**Supplementary Table S2**). Transduction levels on cell lines with variable levels of heparan sulfate proteoglycans (HSPG) (CHO versus pgsA, deficient in all glycosaminoglycans[22]) and sialic acid (Pro5, a derivative of wtCHO, versus Lec2, a Pro5 mutant deficient

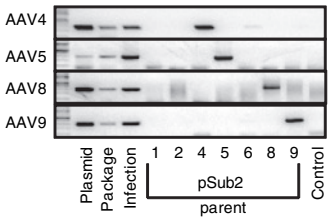

Figure 3 PCR screen of plasmid and viral library. PCRs were performed with serotype-specific primers annealing ~1,400 base pairs (bp) and ~1,700 bp downstream from the *cap* start codon for the forward and reverse primers, respectively. Positive PCRs yield a band of 200–300 bp in size, depending on the serotype. The plasmid library and vector genome DNA from the packaged virus and passaged virus were analyzed along with the individual parent pSub2 plasmids (labeled 1, 2, 4, 5, 6, 8, and 9). AAV, adeno-associated virus.

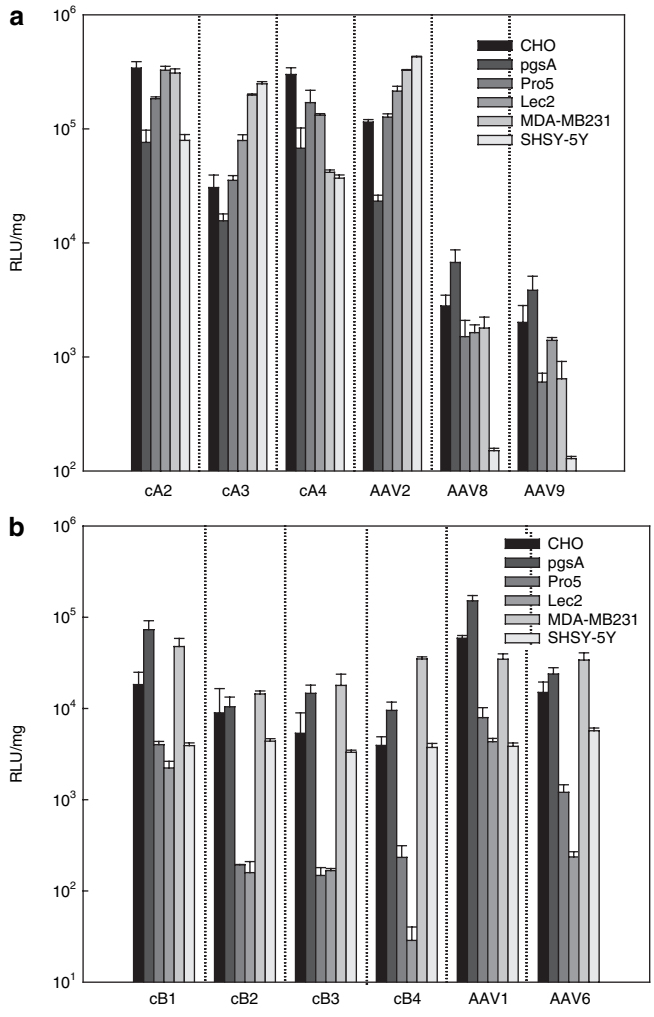

Figure 4 Transduction efficiencies of chimeras and viral parents. rAAV-Luc vectors were used to transduce a panel of cell lines: CHO, pgsA (lacking all GAGs), Pro5, Lec2 (lacking sialic acid), a breast cancer cell line (MDA-MB231), and a neuroblastoma cell line (SHSY-5Y). (**a**) Relative luciferase signals were normalized to total protein (RLU/mg) for AAV2-related chimeras along with AAV2, 8, and 9 controls (n = 3). (Note: cA1 packaged but was noninfectious.) (**b**) Normalized relative luciferase values for AAV1/6-related chimeras along with AAV1 and 6 controls are shown (n = 3). AAV, adeno-associated virus; RLU, relative luciferase unit.

in sialic acid[13]), as well as breast cancer (MDA-MB231) and neuroblastoma (SHSY-5Y) cell lines showed a wide range of tropisms and gene-delivery efficiencies among the chimeras and parents (**Figure 4**). Of the eight clones, only cA1 was noninfectious, likely due to a R238G mutation previously shown to render AAV2 noninfectious,[33] and it thus was not further analyzed. Within the AAV2-like chimeras, tropism varied significantly on cells lacking HSPG (CHO versus pgsA) (**Figure 4**). Within the AAV1/6-like chimeras, cB1, cB3, and cB4 demonstrated slightly but statistically enhanced infection of cells lacking HSPG, suggesting that the lack of this GAG may facilitate infectivity. Interestingly, cB2 and cB3 infections were insensitive to sialic acid (Pro5 versus Lec2), indicating the absence of a sialic acid–binding region despite AAV6's ability to bind sialic acid.[13] Chimera infectivity also varied significantly on two cancer cell lines (*e.g.*, cB2 versus cB1, 3, 4 and AAV1/6) (**Figure 4**). Also of note, neither AAV8 nor AAV9 was sensitive to the lack of HSPG or sialic acid, suggesting these molecules do not serve as receptors for these two recently identified serotypes.[8]

Antibody neutralization

IVIG is purified human IgG derived from the pooled human plasma of ~100,000 individuals. Previous studies showed that IVIG strongly neutralized AAV1–3, 5, and 6, and weakly neutralized AAV4 and 8 (refs. 34,35). To further probe the extent of surface diversity among the new chimeras, as well as to determine whether shuffled capsids can offer additional opportunities for immune evasion and vector re-administration, we determined the IVIG neutralization properties of each. All rAAV green fluorescent protein vectors with chimeric capsids exhibited vector genome-to-transducing units ratios comparable to the respective parent(s) with the exception of cA4, which was approximately tenfold higher than AAV2 (**Supplementary Figure S4**). The IVIG neutralization curves were then measured. Intriguingly, most chimeras were more resistant to antibody neutralization than any of their parents (**Table 1** and **Supplementary Figure S5**), without selection of the library for antibody evasion. Impressively, cB4 was 2-, 8-, and 400-fold more resistant to IVIG neutralization than AAV6, AAV1, and AAV2, respectively. In addition, cA4 was tenfold more resistant to neutralization than AAV2. Interestingly, cB2 was 2.4- and 10-fold more readily neutralized than AAV1 and AAV6, respectively.

In vivo gene delivery

To further demonstrate the gene-delivery potential of these novel chimeras, we analyzed the systemic gene-delivery properties of one highly diverse chimera, cA2, which contains surface loop regions from multiple AAV parent serotypes that exhibit distinct *in vivo* gene-delivery properties. Tail vein injection of rAAV-Luc vectors (10^{11} vector genomes) with capsids from AAV2, 8, and cA2 revealed highly efficient liver and heart transduction by cA2 compared to AAV2, as well as enhanced hindlimb muscle transduction (**Figure 5**). In summary, the novel chimeras exhibit a spectrum of neutralization properties and cell tropisms, highlighting how variations in the external capsid structure can translate into novel gene-delivery properties distinct from the parent serotypes.

Table 1 IVIG neutralization assay of viral chimeras and parent serotypes

Virus	Conc IVIG (mg/ml) for 50% neutralization	Fold resistance relative to parent serotype(s)
cA2	0.095	4.0
cA3	0.097	4.0
cA4	0.27	11.3
AAV2	0.024	—
cB1	1.9	1.6/0.41
cB2	0.49	0.41/0.11
cB3	1.6	1.3/0.35
cB4	9.7	8.1/2.1
AAV1	1.2	—
AAV6	4.6	—

Human intravenous immunoglobulin was used to neutralize recombinant adeno-associated virus (recombinant AAV) green fluorescent protein vectors with capsids from each chimera or parent serotype (n = 3). The intravenous immunoglobulin (IVIG) concentration (mg/ml) required to reduce gene-delivery efficiency to 50% of that in the absence of IVIG is shown. The fold resistance compared to AAV2 (for cA1-4 chimeras) and compared to AAV1/6 (for cB1-4) is shown. All chimeras required significantly higher IVIG concentrations to be neutralized compared to their parent serotypes, with the sole exception of chimera cB2. It should be noted that while the interior of the capsids for these variants were derived from the parent serotype, their external loops often came from other serotypes (**Figure 2**).

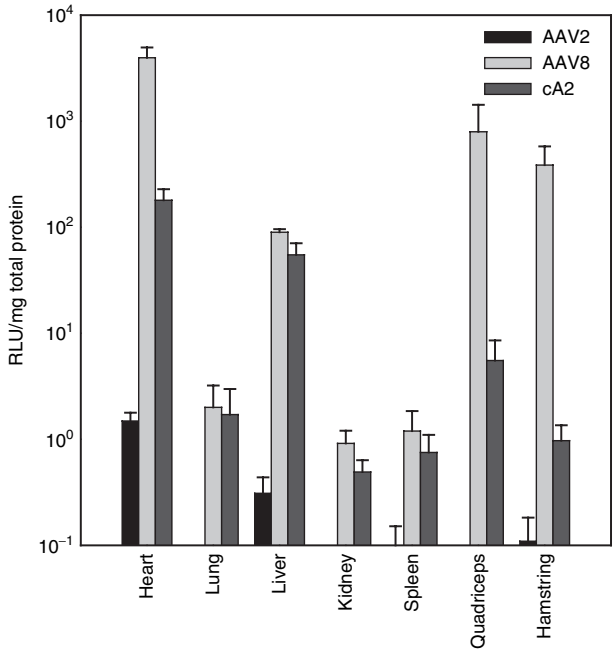

Figure 5 *In vivo* biodistribution transduction efficiencies of chimera and viral parents. rAAV-Luc vectors (10^{11} vector genomes) were delivered via tail vein injections to BALB/c mice (n = 3). For each vector and each tissue analyzed, levels of luciferase expression were normalized to total protein (RLU/mg). AAV, adeno-associated virus; RLU, relative luciferase unit.

DISCUSSION

Recently isolated AAV serotypes possess a diverse range of gene-delivery properties.[10–14] These natural serotypes may not exhibit desirable properties such as efficient transduction of specific cell types or resistance to pre-existing immunity; however, these parents do provide valuable starting material for creating vast numbers of AAV chimeras with new properties. High-throughput selection of these combinatorial AAV chimeras can potentially isolate variants with key properties. Our initial aim was to explore the extent to which highly chimeric viruses from a large (10^7), diverse AAV library of chimeric viruses with regions from multiple AAV serotypes (1, 2, 4–6, 8, and 9) can assemble, package DNA, transduce cells, and exhibit properties distinct from the parent viruses. We therefore applied a low stringency selection for efficient viral packaging and infection, though infection of cultured cells may enrich for clones that use HSPG.[30] To minimize this bias, we performed only a single round of *in vitro* infection. After this selection, seven of eight chimeras analyzed packaged high titer, infectious rAAV with novel gene-delivery properties (**Figures 4** and **5**, and **Table 1**).

Identification of capsid regions that influence cell tropism: The HSPG binding domain of AAV2 has been mapped to the threefold peak of the icosahedral capsid,[36,37] making this region the primary focus of efforts to engineer targeted AAV vectors.[17–19] However, recent evidence demonstrates that capsid regions outside of this peak significantly influence viral infection.[36,37] Correlating the chimeric viral sequences with their transduction properties can identify capsid regions potentially involved in specific viral functions, such as receptor binding. In particular, this analysis implicates several important domains within the parent serotypes, as well as confirms existing functional domains within AAV2. For example, cA2 and cA4, which exhibit novel tropism compared to AAV2 (**Figure 4**), contain amino acids in loop 1 (aa262–270, shown with a white arrow in **Figure 2**) from AAV6 rather than AAV2. This swap results in two sequence changes within the putative fibroblast growth factor receptor–binding region of AAV2 (ref. 36), Q263A and a threonine insertion after aa264, which our results indicate are sufficient to modulate tropism (**Figure 4**).

Unlike the other AAV2-like chimeras, cA2 exhibited a stronger preference for breast cancer cells similar to AAV8. cA2 contains a 99-aa stretch from AAV8, which encompasses two surface loops, loop 2 (aa327–332) and loop 3 (aa381–390), located at the fivefold cylinder and the side of threefold plateau, respectively (indicated by white arrows in **Figure 2**).[38] Interestingly, this region differs from two regions of the AAV8 capsid recently implicated in binding to the laminin receptor.[39] Our results therefore suggest that loops 2 and 3 from AAV8 confer specificity for an alternate receptor or otherwise modulate the viral transduction. Furthermore, swapping of loops 2 or 3 from AAV8 into AAV2 fails to alter liver transduction *in vivo*,[40] suggesting that other loop regions of cA2—such as those inherited from AAV6 (loop1) or AAV9 (~80 aa, including loop 9)—enhance liver transduction by cA2 (**Figure 5**). The enhanced heart and muscle transduction by cA2 may also result from inheriting loop regions from AAV6, 8, and 9, all of which transduce heart and muscle significantly better than AAV2 (refs. 10,12).

Similar analysis of the AAV1/6-like clones implicates potential residues and regions critical for sialic acid binding. For example, cB1 and AAV1 share a weaker sialic acid dependence than cB4 and AAV6 (**Figure 4**). Interestingly, the only difference between cB1 and cB4, which share AAV1/6 sequence in all surface loops, is residue 531 (E in AAV1 and K in AAV6, shown by white arrow in **Figure 2**). This analysis suggests that in addition to conferring

HSPG binding to AAV6 (ref. 41), this residue may also confer enhanced sialic acid dependence.

Chimeras cB2 and cB3 show no dependence on sialic acid for transduction, despite containing a majority of AAV1/6 sequence within the loops[38] and hypervariable regions.[8] The only surface loop of cB2 or cB3 that differs in sequence from cB1 and cB4 is loop 2 (shown by white arrow in **Figure 2**), at two amino acid locations: 325 (T in AAV1/6 versus Q in chimeras) and 329 (V in AAV1/6 versus T in chimeras). This location may facilitate AAV1/6 binding to a sialylated protein receptor, such that these two amino acid changes may disrupt receptor binding and thus alter sialic acid dependence, as supported by the lower transduction relative to AAV1/6 on the parent cell line (Pro5). The functional regions identified from chimeras will facilitate and expedite mutagenesis studies aimed at fully mapping receptor-binding sites or other properties of the AAV serotypes. Finally, it should be noted that the influence of the unique regions of VP1 and VP2 on transduction cannot be discounted, because functional domains involved in intracellular transport[42,43] have been mapped to these locations.

Identification of capsid regions influencing antigenicity: Previous studies have shown that AAV serotypes 1–6 and 8 exhibit variable sensitivity to neutralization by IVIG,[34,35] therefore, examining the IVIG neutralization properties of each chimera serves as an additional probe of their structural and functional differences from the parent serotypes. Furthermore, highly resistant chimeras potentially have strong utility for single-dose gene delivery, but subsequent humoral immune response will likely prevent repeated dosing, unless transient immunosuppression is employed.

The novel chimeras exhibited a broad range of neutralization properties, most with enhanced resistance to IVIG. Chimeras cA2 and cA3, which exhibited a fourfold resistance to IVIG compared to AAV2, contain a C-terminal ~80-aa stretch from AAV9, which maps to the twofold depression previously shown to contain neutralizing epitopes for AAV2 (ref. 15). In addition, mutations within this region enhance resistance to anti-AAV antibodies.[29,36] Interestingly, the cA4 chimera, which contains a V709I mutation and the final 19 aa from AAV6, exhibits a tenfold higher resistance to IVIG compared to AAV2. Most likely, antibody binding to this epitope disrupts AAV binding to its protein receptor, because the epitope is adjacent to the putative fibroblast growth factor receptor–binding domain for AAV2 (ref. 36).

Within the AAV1/6-like chimeras, cB4 is strikingly over 400-fold more resistant to IVIG than AAV2, making it among the most resistant AAV serotypes and variants identified to date.[29,34,35] It is also twofold more resistant than AAV6, likely due to the Y706H mutation within the antigenic twofold depression. By contrast, chimera cB2 was neutralized to a greater extent than AAV1 or 6 by ~2.5-fold and ~10-fold, respectively. cB2 contains a region (aa326–340) shown to contain neutralizing epitopes for AAV2 (ref. 15), potentially making this chimera susceptible to anti-AAV2 antibodies.

Analysis of viable crossover locations: Structure-based analysis of chimeric proteins and recombination sites has identified a constraint upon the location of crossover points: the retention of correct protein folding.[44,45] In particular, chimeric proteins have been found to be more likely to fold and function correctly if key structural contacts are preserved, or inherited from the same parent. The intricate 60-mer AAV capsid offers additional constraints in the regions where several monomers must interact and fold together.[38,46,47] The pentamer formation at the fivefold axis relies mostly on conserved residues with the β-barrel core (AAV2 aa250–253, 371–373, and 654–668) with more minor interactions from loop 2 and loop 9. Thus, crossover locations that combine loop 2 and loop 9 from different serotypes may well be tolerated, because the dominant, conserved β-barrel interactions would offset minor perturbations in loop interactions. Indeed, four of the eight chimeras combined regions of loops 2 and 9 from different serotypes. Likewise, at the twofold axis, the association of two monomers relies predominantly on residues from the β–barrel core, conserved α helix (aa293–302) and loop 9, suggesting that swapping of loop 9 between serotypes may be well tolerated. In fact, three of the eight chimeras contained loop 9 from a serotype different from the one that contributed the β–barrel core.

The most structurally intricate capsid monomer interactions occur at the threefold peak, where two loops from one monomer (aa430–478 and aa577–595) intertwine with two loops from another monomer (aa485–516 and aa539–558) to fold into the final spike conformation. Crossover locations that mix these loops from different serotypes would likely be less tolerated, because extensive complementary structural changes in adjacent hypervariable loops are likely required to assemble this capsid interface properly.[38,46,47] For example, a previous study of AAV1-AAV2 chimeras showed tenfold lower particle yields for chimeras swapping residues 481–564 or 565–669 (ref. 21). Intriguingly, all the chimeras in this study inherited all four loops from a single parent (**Figure 2**). Future efforts to create novel AAV chimeras may have to account for these complex subunit interactions, particularly at the threefold peak, to ensure efficient viral assembly.

Implications for future work: We have generated a large, functionally diverse AAV library through DNA shuffling of the *cap* genes from numerous parent serotypes. Furthermore, this library contains chimeras with broad diversity in cell tropism and neutralizing antibody resistance. This approach can therefore successfully harness and blend functions from newly identified AAV serotypes, or even rationally designed mutants, to potentially create a combinatorially limitless number of novel variants with new properties. Coupled with efficient selections,[29] this forward genetics approach has the potential to evolve novel AAV vectors with customized gene-delivery properties for many applications, and reverse engineering of the results will further enhance our knowledge of the basic structure–function relationships for the AAV capsid.

MATERIALS AND METHODS

Library construction. *cap* genes from AAV1, AAV2, AAV4, AAV5, AAV6, AAV8, and AAV9 were amplified by PCR with primers that introduced unique sites for *Hin*dIII (5′) and *Not*I (3′) and individually cloned into the AAV2 genome plasmid pSub2 (ref. 29). Each viral *cap* gene was then amplified via PCR using 5′-CATGGGAAAGGTGCCAGACG-3′ and 5′-CGCAGAGACCAAAGTTCAACTGA-3′ as forward and reverse primers, respectively. DNA shuffling was performed as previously described.[23,32] Briefly, equimolar amounts of PCR-amplified *cap* genes (1–3 μg total DNA) were digested with DNase I (Roche, Indianapolis, IN) for varying times (5–20 minutes) to yield fragments ranging from 50 to 500 base pairs

in size. Fragments were gel purified, and 10–20 µl of purified DNA was reassembled in a PCR containing 1× ThermoPol buffer (NEB), 200 µmol/l deoxynucleotide triphosphates, and 1 unit Vent DNA polymerase (NEB) under the following conditions: 96 °C, 3 minutes; 40 cycles of 94 °C, 1 minute; 55 °C for 1 minutes; 72 °C for 1 minute + 4 seconds/cycle; and 72 °C, 10 minutes. Assembled fragments were further amplified using the same reaction conditions as above with the above primers, and chimeric *cap* genes containing unique *Hin*dIII (5′) and *Not*I (3′) sites were cloned into pSub2 for rcAAV production.

Cell lines and viral production. Unless otherwise mentioned, cell lines were obtained from the American Type Culture Collection (Manassas, VA) and cultured at 37 °C and 5% CO_2. HEK293T, CHO K1, and CHO pgsA were cultured in Iscove's modified Dulbecco's medium (Mediatech, Herndon, VA). Pro5 and Lec2 were cultured in minimum essential medium, α-modification (Sigma-Aldrich, St Louis, MO). MDA-MB231 and SHSY-5Y were cultured in Dulbecco's modified Eagle's medium with 1% nonessential amino acids (Invitrogen, Carlsbad, CA). AAV293 cells (Stratagene, La Jolla, CA) were cultured in Dulbecco's modified Eagle's medium. All media were supplemented with 10% fetal bovine serum (Invitrogen) and 1% penicillin/streptomycin (Invitrogen).

The rcAAV library and rAAV vectors were packaged as previously described.[29,48] Briefly, for the rcAAV library, AAV293 cells grown in a 15-cm plate were transfected with 7 ng rcAAV library, 25 µg pBluescript, and 25 µg pHelper. Forty-eight hours after transfection, the resulting viral library was harvested and titered via quantitative PCR to obtain DNase-resistant genomic titers or flow cytometry to obtain transduction titers as previously described.[29,48]

In vitro ***selection and characterization.*** To recover functional shuffled virions, 3×10^6 293T cells were infected with the AAV library at a genomic multiplicity of infection of 50, and AAV was amplified or rescued by infection with wild-type adenovirus serotype 5 (Ad5) as previously described.[29] Viral genomic DNA was recovered by PCR amplification.

PCR screens were performed with 10 ng of template from the plasmid library, viral genomic DNA, or the pSub2 plasmid for each serotype. Serotype sequence primers (**Supplementary Table S1**) were used along with Taq DNA polymerase in a PCR program of 95 °C for 30 seconds; 95 °C for 30 seconds, 55 °C for 30 seconds, and 72 °C for 20 second (35 times); and 72 °C for 10 minutes.

To determine the relative transduction efficiencies of each clone compared to the parent viruses, 5×10^4 cells were infected with rAAV vectors carrying complementary DNA encoding firefly luciferase at a genomic multiplicity of infection of 10^4. Forty-eight hours after infection, cells were rinsed with phosphate-buffered saline, and luciferase assays were performed as previously reported.[49] The luciferase signal was normalized to total protein content determined by a BCA assay (Pierce, Rockford, IL).

In vitro ***neutralization assay with IVIG.*** Antibody neutralization assays were performed as reported.[29] Briefly, rAAV green fluorescent protein vectors were incubated with varying levels of human IVIG (Bayer) in a 75 µl final volume for 30 minutes at 20 °C, followed by addition to 2.5×10^5 293T cells at a multiplicity of infection of 1. After 48 hours, the fraction of fluorescent cells was quantified by flow cytometry.

In vivo ***gene delivery.*** Recombinant AAV vectors carrying the complementary DNA for firefly luciferase under the control of the CMV promoter without the β-globin intron were produced. High-titer AAV2, AAV8, and cA2 vectors were produced and purified via iodixanol density ultracentrifugation followed by dialysis as previously described.[29] Approximately 10^{11} DNase-resistant particles were injected into the tail vein of 8-week-old female BALB/c mice (Jackson Laboratories, Bar Harbor, ME; $n = 3$). Four weeks after injection, animals were killed, and representative organs (lung, liver, heart, kidney, spleen, quadriceps, and hamstring) were harvested and frozen. Frozen tissue samples were homogenized in reporter lysis buffer (Promega, Mannheim, Germany) and clarified by centrifugation for 10 minutes at 10,000*g*. Luciferase reporter activities were determined as previously described,[49] and the luciferase signal was normalized to total protein content determined by a bicinchoninic acid assay (Pierce). Animal protocols were approved by the UCB Animal Care and Use Committee and conducted in accordance with National Institutes of Health guidelines.

SUPPLEMENTARY MATERIAL

Figure S1. Graphic representation of DNA sequences from several random clones within the plasmid library.
Figure S2. Graphic representation of DNA sequences from the eight chimeras chosen for analysis.
Figure S3. Primary amino acid sequence alignment of VP1 proteins from AAV1, 2, 4-6, 8, 9 and the eight chimeras.
Figure S4. Genomic:transducing particle ratios for rAAV GFP vectors packaged with each chimeric or parent capsid.
Figure S5. Full neutralization curves for rAAV GFP vectors with chimeric or parent capsids.
Table S1. Primer sequences for AAV serotype PCR screen.
Table S2. DNase-resistant particle titers for rAAV Luc vectors packaged with each chimeric or parent capsid as determined by quantitative PCR.

ACKNOWLEDGMENTS

We thank Lindsey Jennings for technical help with the animal work. This work was supported by UC Discovery BIO05-10559 and BIO07-10646, a NSF Graduate Fellowship (to J.T.K.), training grant T1-00007 from the California Institute for Regenerative Medicine, and NIH R01 HL081527.

REFERENCES

1. Verma, IM and Weitzman, MD (2005). Gene therapy: twenty-first century medicine. *Annu Rev Biochem* **74**: 711–738.
2. Manno, CS, Pierce, GF, Arruda, VR, Glader, B, Ragni, M, Rasko, JJ *et al.* (2006). Successful transduction of liver in hemophilia by AAV-Factor IX and limitations imposed by the host immune response. *Nat Med* **12**: 342–347.
3. Maguire, AM, Simonelli, F, Pierce, EA, Pugh, EN Jr., Mingozzi, F, Bennicelli, J *et al.* (2008). Safety and efficacy of gene transfer for Leber's congenital amaurosis. *N Engl J Med* **358**: 2240–2248.
4. McCown, TJ, Xiao, X, Li, J, Breese, GR and Samulski, RJ (1996). Differential and persistent expression patterns of CNS gene transfer by an adeno-associated virus (AAV) vector. *Brain Res* **713**: 99–107.
5. Kaplitt, MG, Leone, P, Samulski, RJ, Xiao, X, Pfaff, DW, O'Malley, KL *et al.* (1994). Long-term gene expression and phenotypic correction using adeno-associated virus vectors in the mammalian brain. *Nat Genet* **8**: 148–154.
6. Lai, K, Kaspar, BK, Gage, FH and Schaffer, DV (2003). Sonic hedgehog regulates adult neural progenitor proliferation *in vitro* and *in vivo*. *Nat Neurosci* **6**: 21–27.
7. Srivastava, A, Lusby, EW and Berns, KI (1983). Nucleotide sequence and organization of the adeno-associated virus 2 genome. *J Virol* **45**: 555–564.
8. Gao, G, Alvira, MR, Somanathan, S, Lu, Y, Vandenberghe, LH, Rux, JJ *et al.* (2003). Adeno-associated viruses undergo substantial evolution in primates during natural infections. *Proc Natl Acad Sci USA* **100**: 6081–6086.
9. Chiorini, JA, Kim, F, Yang, L and Kotin, RM (1999). Cloning and characterization of adeno-associated virus type 5. *J Virol* **73**: 1309–1319.
10. Wang, Z, Zhu, T, Qiao, C, Zhou, L, Wang, B, Zhang, J *et al.* (2005). Adeno-associated virus serotype 8 efficiently delivers genes to muscle and heart. *Nat Biotechnol* **23**: 321–328.
11. Davidson, BL, Stein, CS, Heth, JA, Martins, I, Kotin, RM, Derksen, TA *et al.* (2000). Recombinant adeno-associated virus type 2, 4, and 5 vectors: transduction of variant cell types and regions in the mammalian central nervous system. *Proc Natl Acad Sci USA* **97**: 3428–3432.
12. Inagaki, K, Fuess, S, Storm, TA, Gibson, GA, McTiernan, CF, Kay, MA *et al.* (2006). Robust systemic transduction with AAV9 vectors in mice: efficient global cardiac gene transfer superior to that of AAV8. *Mol Ther* **14**: 45–53.
13. Wu, Z, Miller, E, Agbandje-McKenna, M and Samulski, RJ (2006). Alpha2,3 and alpha2,6 N-linked sialic acids facilitate efficient binding and transduction by adeno-associated virus types 1 and 6. *J Virol* **80**: 9093–9103.
14. Kaludov, N, Brown, KE, Walters, RW, Zabner, J and Chiorini, JA (2001). Adeno-associated virus serotype 4 (AAV4) and AAV5 both require sialic acid binding for hemagglutination and efficient transduction but differ in sialic acid linkage specificity. *J Virol* **75**: 6884–6893.
15. Moskalenko, M, Chen, L, van Roey, M, Donahue, BA, Snyder, RO, McArthur, JG *et al.* (2000). Epitope mapping of human anti-adeno-associated virus type 2 neutralizing antibodies: implications for gene therapy and virus structure. *J Virol* **74**: 1761–1766.
16. Wobus, CE, Hugle-Dorr, B, Girod, A, Petersen, G, Hallek, M and Kleinschmidt, JA (2000). Monoclonal antibodies against the adeno-associated virus type 2 (AAV-2) capsid: epitope mapping and identification of capsid domains involved in AAV-2-cell interaction and neutralization of AAV-2 infection. *J Virol* **74**: 9281–9293.

17. Girod, A, Ried, M, Wobus, C, Lahm, H, Leike, K, Kleinschmidt, J *et al.* (1999). Genetic capsid modifications allow efficient re-targeting of adeno-associated virus type 2. *Nat Med* **5**: 1052–1056.
18. Shi, W, Arnold, GS and Bartlett, JS (2001). Insertional mutagenesis of the adeno-associated virus type 2 (AAV2) capsid gene and generation of AAV2 vectors targeted to alternative cell-surface receptors. *Hum Gene Ther* **12**: 1697–1711.
19. Grifman, M, Trepel, M, Speece, P, Gilbert, LB, Arap, W, Pasqualini, R *et al.* (2001). Incorporation of tumor-targeting peptides into recombinant adeno-associated virus capsids. *Mol Ther* **3**: 964–975.
20. Bowles, DE, Rabinowitz, JE and Samulski, RJ (2003). Marker rescue of adeno-associated virus (AAV) capsid mutants: a novel approach for chimeric AAV production. *J Virol* **77**: 423–432.
21. Hauck, B and Xiao, W (2003). Characterization of tissue tropism determinants of adeno-associated virus type 1. *J Virol* **77**: 2768–2774.
22. Rabinowitz, JE, Bowles, DE, Faust, SM, Ledford, JG, Cunningham, SE and Samulski, RJ (2004). Cross-dressing the virion: the transcapsidation of adeno-associated virus serotypes functionally defines subgroups. *J Virol* **78**: 4421–4432.
23. Stemmer, WP (1994). Rapid evolution of a protein *in vitro* by DNA shuffling. *Nature* **370**: 389–391.
24. Soong, NW, Nomura, L, Pekrun, K, Reed, M, Sheppard, L, Dawes, G *et al.* (2000). Molecular breeding of viruses. *Nat Genet* **25**: 436–439.
25. Boder, ET, Midelfort, KS and Wittrup, KD (2000). Directed evolution of antibody fragments with monovalent femtomolar antigen-binding affinity. *Proc Natl Acad Sci USA* **97**: 10701–10705.
26. Daugherty, PS, Chen, G, Iverson, BL and Georgiou, G (2000). Quantitative analysis of the effect of the mutation frequency on the affinity maturation of single chain Fv antibodies. *Proc Natl Acad Sci USA* **97**: 2029–2034.
27. Zhao, H, Giver, L, Shao, Z, Affholter, JA and Arnold, FH (1998). Molecular evolution by staggered extension process (StEP) *in vitro* recombination. *Nat Biotechnol* **16**: 258–261.
28. Yu, JH and Schaffer, DV (2006). High-throughput, library-based selection of a murine leukemia virus variant to infect nondividing cells. *J Virol* **80**: 8981–8988.
29. Maheshri, N, Koerber, JT, Kaspar, BK and Schaffer, DV (2006). Directed evolution of adeno-associated virus yields enhanced gene delivery vectors. *Nat Biotechnol* **24**: 198–204.
30. Grimm, D, Lee, JS, Wang, L, Desai, T, Akache, B, Storm, TA *et al.* (2008). *In vitro* and *in vivo* gene therapy vector evolution via multispecies interbreeding and retargeting of adeno-associated viruses. *J Virol* **82**: 5887–5911.
31. Li, W, Asokan, A, Wu, Z, Van Dyke, T, Diprimio, N, J, SJ *et al.* (2008). Engineering and selection of shuffled AAV genomes: a new strategy for producing targeted biological nanoparticles. *Mol Ther* **16**: 1252–1260.
32. Zhao, H and Arnold, FH (1997). Optimization of DNA shuffling for high fidelity recombination. *Nucleic Acids Res* **25**: 1307–1308.
33. Wu, P, Xiao, W, Conlon, T, Hughes, J, Agbandje-McKenna, M, Ferkol, T *et al.* (2000). Mutational analysis of the adeno-associated virus type 2 (AAV2) capsid gene and construction of AAV2 vectors with altered tropism. *J Virol* **74**: 8635–8647.
34. Arbetman, AE, Lochrie, M, Zhou, S, Wellman, J, Scallan, C, Doroudchi, MM *et al.* (2005). Novel caprine adeno-associated virus (AAV) capsid (AAV-Go.1) is closely related to the primate AAV-5 and has unique tropism and neutralization properties. *J Virol* **79**: 15238–15245.
35. Lochrie, MA, Tatsuno, GP, Arbetman, AE, Jones, K, Pater, C, Smith, PH *et al.* (2006). Adeno-associated virus (AAV) capsid genes isolated from rat and mouse liver genomic DNA define two new AAV species distantly related to AAV-5. *Virology* **353**: 68–82.
36. Lochrie, MA, Tatsuno, GP, Christie, B, McDonnell, JW, Zhou, S, Surosky, R *et al.* (2006). Mutations on the external surfaces of adeno-associated virus type 2 capsids that affect transduction and neutralization. *J Virol* **80**: 821–834.
37. Opie, SR, Warrington, KH Jr., Agbandje-McKenna, M, Zolotukhin, S and Muzyczka, N (2003). Identification of amino acid residues in the capsid proteins of adeno-associated virus type 2 that contribute to heparan sulfate proteoglycan binding. *J Virol* **77**: 6995–7006.
38. Xie, Q, Bu, W, Bhatia, S, Hare, J, Somasundaram, T, Azzi, A *et al.* (2002). The atomic structure of adeno-associated virus (AAV-2), a vector for human gene therapy. *Proc Natl Acad Sci USA* **99**: 10405–10410.
39. Akache, B, Grimm, D, Pandey, K, Yant, SR, Xu, H and Kay, MA (2006). The 37/67-kilodalton laminin receptor is a receptor for adeno-associated virus serotypes 8, 2, 3, and 9. *J Virol* **80**: 9831–9836.
40. Shen, X, Storm, T and Kay, MA (2007). Characterization of the relationship of AAV capsid domain swapping to liver transduction efficiency. *Mol Ther* **15**: 1955–1962.
41. Wu, Z, Asokan, A, Grieger, JC, Govindasamy, L, Agbandje-McKenna, M and Samulski, RJ (2006). Single amino acid changes can influence titer, heparin binding, and tissue tropism in different adeno-associated virus serotypes. *J Virol* **80**: 11393–11397.
42. Grieger, JC, Snowdy, S and Samulski, RJ (2006). Separate basic region motifs within the adeno-associated virus capsid proteins are essential for infectivity and assembly. *J Virol* **80**: 5199–5210.
43. Girod, A, Wobus, CE, Zadori, Z, Ried, M, Leike, K, Tijssen, P *et al.* (2002). The VP1 capsid protein of adeno-associated virus type 2 is carrying a phospholipase A2 domain required for virus infectivity. *J Gen Virol* **83**: 973–978.
44. Voigt, CA, Martinez, C, Wang, ZG, Mayo, SL and Arnold, FH (2002). Protein building blocks preserved by recombination. *Nat Struct Biol* **9**: 553–558.
45. Otey, CR, Landwehr, M, Endelman, JB, Hiraga, K, Bloom, JD and Arnold, FH (2006). Structure-guided recombination creates an artificial family of cytochromes P450. *PLoS Biol* **4**: e112.
46. Govindasamy, L, Padron, E, McKenna, R, Muzyczka, N, Kaludov, N, Chiorini, JA *et al.* (2006). Structurally mapping the diverse phenotype of adeno-associated virus serotype 4. *J Virol* **80**: 11556–11570.
47. Nam, HJ, Lane, MD, Padron, E, Gurda, B, McKenna, R, Kohlbrenner, E *et al.* (2007). Structure of adeno-associated virus serotype 8, a gene therapy vector. *J Virol* **81**: 12260–12271.
48. Koerber, JT, Jang, JH, Yu, JH, Kane, RS and Schaffer, DV (2007). Engineering adeno-associated virus for one-step purification via immobilized metal affinity chromatography. *Hum Gene Ther* **18**: 367–378.
49. Ignowski, JM and Schaffer, DV (2004). Kinetic analysis and modeling of firefly luciferase as a quantitative reporter gene in live mammalian cells. *Biotechnol Bioeng* **86**: 827–834.
50. Mingozzi, F, Maus, MV, Hui, DJ, Sabatino, DE, Murphy, SL, Rasko, JE *et al.* (2007). CD8(+) T-cell responses to adeno-associated virus capsid in humans. *Nat Med* **13**: 419–422.